ELSEVIER

Contents lists available at ScienceDirect

Resources, Conservation & Recycling Advances

journal homepage: www.sciencedirect.com/journal/ Resources-Conservation-and-Recycling-Advances



Calcium carbonate production from surf clam and ocean quahog shells: Process development and techno-economic analysis

Yanhong He $^{\#},$ Mojtaba Enayati $^{\S,\#},$ Younas Dadmohammadi, Martin Liu, Peilong Li, Alireza Abbaspourrad *

Department of Food Science, College of Agriculture and Life Sciences, Cornell University, 243 Stocking Hall, 411 Tower Rd, Ithaca, NY, 14853, United States of America

ARTICLE INFO

Keywords: Resource recovery Seashells Calcium carbonate Heat treatment Techno-economic analysis Sustainability

ABSTRACT

The conversion of surf clam shells (SCS) and ocean quahog shells (QS) into three different grades of $CaCO_3$ products using water and lower-temperature processing was investigated. Coarsely ground shells were boiled in water for 2 h and then washed and dried, followed by fine grinding and heating. To produce the highest quality of $CaCO_3$, the washed ground shells were processed at 300 °C for 2 h. Process modeling and economic analysis were performed on these three products using SuperPro Designer. For a processing plant with an annual capacity of 10,886 MT of waste shells, the highest grade $CaCO_3$ product had the highest predicted economic performance with a net present value of \$4.3 M, an internal rate of return of 12.7 %, and payback period of 5.6 years. The sensitivity analysis showed plant capacity and selling price were the predominant variables that affected production economic feasibility.

1. Introduction

The growing demand for shellfish, including bivalves and crustaceans, has resulted in a rapid accumulation of waste seashells. Approximately 89 % of bivalves currently consumed are produced by the aquaculture industry while the other 11 % are harvested from the wild (Wijsman et al., 2019). The European Union, U.S., China, and South Korea account are the largest consumers (The State of World Fisheries and Aquaculture 2022, 2022). China, as the top country for shellfish production, generates around ten million metric tons (MT) of waste seashells annually (Mo et al., 2018). From the global perspective, the annual shell wastes could be at least 10-20 million tons (Wang and Liu, 2020). Most of the waste seashells are disposed of in landfills or returned to the sea, constituting a waste of resources and creating economic and environmental hurdles (Hembrick-Holloman et al., 2020). In Australia, for example, the disposal of waste seashells can cost \$150/MT (Yan and Chen, 2015). Additionally, inappropriate disposal of waste seashells leads to offensive odors, when the organic compounds decompose, and sanitation problems, seashells are prime habitats for microorganisms (Aimikhe and Lekia, 2021). These hard protective shells account for 65-90 % (Summa et al., 2022) of live weight, depending on the species and are composed of 95–99 % calcium carbonate ($CaCO_3$) and 1–5 % of the organic matrix (Barros et al., 2009; Tayeh et al., 2019). With the global market for $CaCO_3$ expected to grow at a compound annual growth rate of 5 % between 2020–2026 (ReportLinker, 2022) driven by the increasing consumption of the material from end-use segments, especially paper, plastics, and paints, it is worth investigating sustainable ways to use this abundant and renewable resource (*Global calcium carbonate market 2016–2020*, n.d.).

CaCO₃ exists naturally in three predominate forms: calcite, aragonite, and vaterite (Yadav et al., 2021). Chalk, limestone, and marble are the predominant source rocks mined by the chemicals industry to procure CaCO₃. The two highest value-added products in the limestone value chain are ground CaCO₃ (GCC), and precipitated CaCO₃. GCC is generally mined from large natural deposits of ore (limestone or marble); in 2020, it occupied 82 % of the CaCO₃ market (*Global calcium carbonate market 2016–2020*, n.d.). Although modern mining technology has improved, mining activities inevitably impact the environment by increasing air and water pollution, harming wildlife and scarring the landscape (Ganapathi and Phukan, 2020). The rising concerns regarding mining of carbonate rock resources hampers the market growth of CaCO₃ (Ganapathi and Phukan, 2020). Consequently, a high-quality,

https://doi.org/10.1016/j.rcradv.2023.200190

 $^{^{\}ast}$ Corresponding author.

E-mail address: alireza@cornell.edu (A. Abbaspourrad).

[#] These authors contributed equally to the work described in this manuscript.

[§] Present Address: Center for Materials and Manufacturing Sciences, Departments of Chemistry and Physics, Troy University, Troy, AL, 36082, USA.

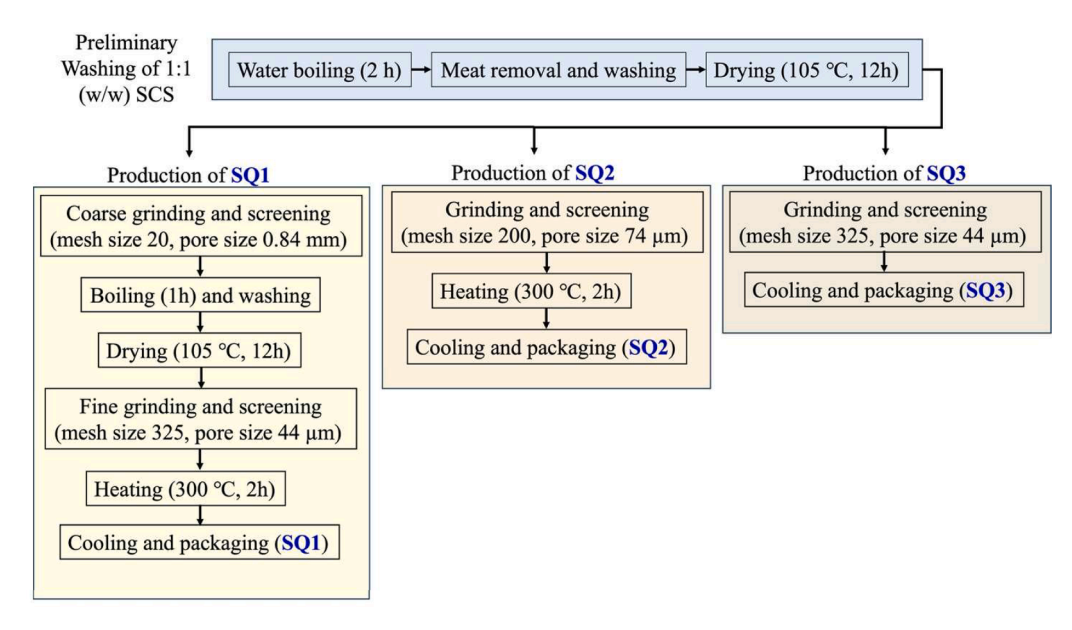


Fig. 1. Process flow diagrams of the production of three CaCO₃ products (SQ1, SQ2, and SQ3) from the mixture of waste shells of surf clam (SCS) and ocean quahog (QS).

environmentally friendly, and economical source of ${\rm CaCO_3}$ to reduce the dependence on traditional carbonate is needed.

Previous work has shown that the CaCO3 in seashells can be harvested and used in a variety of applications. For example, CaCO₃ from milled oyster and mussel shells followed by heating at 500 °C for 2 h is a suitable replacement for fillers in polypropylene (Hamester et al., 2012). Similarly, CaCO₃ obtained from varied mollusks such as cockles, wedge-shells, and other small bivalve shells, can also be used as fillers in polymer matrices; in this case the processing of the CaCO3 included washing the seashells with 4 % sodium hydroxide solution for 24 h, then drying them at 100 °C before grinding (Fombuena et al., 2014). Another process for processing the CaCO3 derived from oyster shells requires treating them with sodium hydroxide, hydrochloric acid, sodium carbonate, and drying at 100 °C (Lin et al., 2020). The resulting material from this process was used as an adsorbent for removing heavy metals in contaminated water. Further, washed oysters and clamshells were washed with a biodegradable detergent, dried, and used to produce CaCO₃ suitable for the incorporation into construction materials and a residential wall finish (Águila-Almanza et al., 2022). Recently, precipitated calcium carbonate was produced by calcinating green mussel shells at 900 °C for 5 h followed by carbonation (Prihanto et al., 2022). However, these processing usually involved the use of chemicals and/or high calcination temperatures. Therefore, developing a process that does not require toxic chemicals and uses a low heating temperature would benefit both the environment and the economy.

While CaCO3 derived from mussel shells has been used as mulches for soil amendment in farming, as cattle beds, and additive in poultry feed (Barros et al., 2009), little information on the production and quality of the CaCO3 products obtained or a detailed analysis of their techno-economic impact for commercial-scale production could be found. To address this gap in the literature, we (1) developed processes to recover CaCO₃ from waste shells of surf clam (SCS) and ocean quahog (QS), which are two species of clams with the highest populations in the United States (Fisheries, 2022); and (2) conducted techno-economic analysis (TEA) to evaluate the economic feasibility of the developed technology. We compared the effects of various preparation and isolation processes on the quality of our CaCO3 seeking a low energy, environmentally friendly process for a scaled-up production. The results from both lab-scale and scaled-up processes were used as a basis for our TEA. To our knowledge, this is the first study to produce different grades of CaCO₃ products from SCS and QS using only water and a low heating temperature. We also performed a TEA analysis to evaluate the viability of commercial production. The results of this work will provide the aquaculture industry with a baseline on which to direct their waste shell management.

2. Materials and methods

2.1. Materials

Shell samples (SCS and QS) were provided by seafood processing companies on the East coast of the United States, including Surfside Foods LLC (NJ), Atlantic Capes Fisheries, Inc. (NJ), La Monica Fine Foods (NJ), Sea Watch International, Ltd. (MD). The samples were stored at -18 $^{\circ}$ C before use. Standard calcium carbonate (99 %, extra pure, Thermo Scientific) was used as received.

2.2. Lab-scale production of CaCO3 from SCS and QS

The production of $CaCO_3$ from shells was done in two steps, cleaning and drying of the whole shells, followed by grinding, boiling in water and heating. The initial cleaning step was carried out using thawed raw waste shells (SCS and QS) (**Figure S1**) that were separated and prewashed with tap water to remove impurities, such as salts, dirt, and remaining separable meats. The whole shells were then dried in an oven at 70 °C for 12 h.

The cleaned shells were roughly ground to a particle size of 5–10 mm using a porcelain mortar and pestle, the ground shells were boiled in deionized water for two hours and then washed with deionized water. The washed ground shells were oven dried at 70 $^{\circ}\mathrm{C}$ for 12 h.

To study the effect of heating temperature and shell particle size on the physical and chemical properties of the $CaCO_3$ produced, three different particle sizes, 5–10 mm, 0.5–5 mm and 40–80 μm , were produced and samples from each were heated at 300, 350, and 500 $^{\circ}C.$ Particle sizes of 5–10 mm were prepared using a mortar and pestle, while 0.5–5 mm particles were obtained using a coffee grinder, and finally, micrometer -size shells were prepared using an MSK-SFM-3 desktop high-speed vibrating ball mill (Richmond, CA, USA) by placing $\sim\!\!50$ g of washed coarsely ground shells into the metal chamber with stainless steel balls and milling for 30 min.

The color and calcium carbonate content of the final products in each temperature and particle size test was used to find the best conditions for

scale up and plant design. Grinding the shells to the micrometer size before heating at 300 $^{\circ}$ C was found to produce the highest calcium carbonate content with the whitest color.

2.3. Production of three different grades of CaCO₃.

Based on the lab-scale results, the heating step was limited to 300 $^{\circ}$ C and three grades of CaCO₃ were made each of which targeted different potential applications including animal feed, paper, and agricultural/construction (Fig. 1).

The same initial cleaning step was undertaken for each grade where a 1:1 (w/w) mixture of SCS and QS shells were first boiled in deionized water for 2 h, meat and debris were removed followed by water wash and then oven dried at 105 °C for 12 h. Three separate processes were then used to produce different grades of CaCO3: SQ1, SQ2, and SQ3 (Fig. 1). SQ1 was produced by boiling the shells with particle size 0.84 mm for an hour and drying, then fine grinding to 44 μm and heating at 300 °C for two hours. Samples of SQ2 were prepared by grinding the washed shells to 74 μm and then heating at 300 °C for two hours. Finally, samples of SQ3 were produced immediately after cleaning by grinding to 44 μm and screening the particles for uniformity; SQ3 samples were not heated to 300 °C. The produced samples were stored at room temperature for further analysis.

2.4. Physicochemical characterization of CaCO₃ products

241 Color

Color parameters of $CaCO_3$ samples, including L* (degree of lightness), a* (degree of redness (+) and greenness (-)), and b* (degree of yellowness (+) and blueness (-)) were measured with a portable Konica Minolta CR-400 colorimeter (Tokyo, Japan). A standard calibration whiteboard was used to calibrate the colorimeter before measurement.

2.4.2. In vitro solubility, loose bulk density, and pH

In vitro solubility of CaCO $_3$ samples was determined using a weight loss method reported by Kim et al. (2018) with modification. Briefly, 40 mL of 0.2 N HCl was mixed with 0.4 g sample in a 50 mL centrifuge tube and incubated in a water bath at 42 °C, with mixing at 150 rpm for 10 min. The mixture was then vacuum filtered through a 2.5 μ m Whatman filter paper. The filter paper was dried at 100 °C for 24 h and the remaining solids weighed. The weight difference was used for the solubility calculation. The Loose bulk density was determined by measuring the mass of a known volume of samples. The pH measurement was performed according to ASTM C25 (ASTM C25, 2021). Briefly, 1 g of the sample and 20 mL CO $_2$ -free deionized water with 200 rpm at 25 °C for 30 min. The mixture was left to stand for 30 min to allow the suspended material to settle out from the suspension, then the pH of the supernatant was measured.

2.4.3. X-ray diffraction

The crystal structure of the samples was determined by X-ray diffraction (XRD) analysis, which was conducted using a Bruker D8 Advance eco powder diffractometer (Billerica, MA, USA) with Cu K α radiation. Diffractograms were collected in the 2θ range of $15-70^{\circ}$ at a scanning rate of 1.3° min $^{-1}$, and the step size was 0.02° The divergent beam slit was 0.1 mm and detector slit was 3 mm.

2.4.4. Fourier transform infrared spectroscopy

Fourier transform infrared spectroscopy (FTIR) was conducted with an ATR-FTIR (Affinity-1S, Shimadzu, Kyoto, Japan) to assess changes in chemical bonds in $CaCO_3$ samples. Samples were scanned from 400 to $4000~\rm cm^{-1}$ in a transmittance mode with a 4 cm⁻¹ resolution and 64 scans.

2.4.5. Scanning electron microscopy

The morphology of the clean, dried, and ground surf clam and

quahog shell particles were examined using scanning electron microscopy (SEM) (Zeiss Gemini 500, Germany). Dry samples were coated with Au-Pd using a sputter coater (Denton Desk V, NJ, USA) for 40 s at 30 mA and 2×10^{-4} mbar. Coated objects were scanned with 1 keV and imaged by a high efficiency secondary electron detector with a 20.0 μm aperture.

2.4.6. Elemental composition (X-ray fluorescence)

Elemental analysis was performed in the Materials Analysis and Research Lab at Iowa State University (Ames, IA, USA) using a PANalytical PW2404 X-ray fluorescence spectrometer (XRF) with 45 kV, 66 mA and 2970 W, and Analytical Chemistry Research Laboratory at the Virginia Maryland College of Veterinary Medicine (Blacksburg, VA, USA) using an inductively coupled plasma mass spectrometer (Agilent 7900 ICP-MS). Pellets for XRF were prepared according to our standard procedure: to 8 g of dried sample, 1 g of boric acid was added, then to two separate samples of this mixture (\sim 500 mg each) was added 2 g of ChemplexTM X-ray Mix Powder (Cat. No. 600). This mixture was further ground for 2 minutes in a ShatterboxTM to ensure thorough blending. Then 40 mm diameter pellets were pressed under a 25-ton load for 30 seconds in a hydraulic press. In addition to our samples, a control sample of reagent grade calcium carbonate was similarly prepared for comparison.

2.4.7. CaCO₃ content determination

The thermal decomposition behavior and the amount of $CaCO_3$ content in the produced samples were determined using thermogravimetric analysis (TGA) performed on a TGA Q500 (TA instrument Inc, USA), between 25 and 950 °C at a heating rate of 10 °C min⁻¹. $CaCO_3$ decomposed within the temperature range of 650–915 °C (Ferraz et al., 2019). The $CaCO_3$ content was calculated using Eq. (1).

CaCO₃ content (%) =
$$\frac{(W_{650 \cdot C} - W_{915 \cdot C}) \times 2.274}{W_{25 \cdot C}} \times 100\%$$
 (1)

where, $W_{650 \cdot C}$, $W_{915 \cdot C}$, and $W_{25 \cdot C}$ are the weights of CaCO₃ samples at temperatures of 650, 915, and 25 °C respectively; 2.274 is the molar mass conversion factor (ratio of the molar mass of CaCO₃ (100.09 g/mol) to CO₂ (44.01 g/mol)).

2.4.8. Statistical analysis

One-way analysis of variance (ANOVA) and Tukey's HSD (honestly significant difference) were performed using JMP Pro16 (SAS, Cary, NC, USA). Differences were considered significant when p < 0.05.

2.5. Techno-economic analysis of CaCO₃ production

Techno-economic analysis (TEA) is a systematic way to evaluate the technical and economic viability of a designed process by combining process modeling, engineering design, mass-energy balance, and economic evaluation. The TEA model for CaCO₃ production was conducted using SuperPro Designer v12 (Intelligen, Inc., Scotch Plains, NJ, USA). A survey was designed to collect information about SCS and QS production and the location of shell processing plants. The survey was distributed via email and a Google Form link to the members of the Science Center for Marine Fisheries (Mississippi, USA). The information collected from this survey was used to determine the plant capacity and plant location for process simulation with SuperPro Designer software. Considering the cost of waste seashells transportation, it was assumed that the CaCO3 production plant would be co-located at a large bivalve processing plant that can store the seasonal collected waste seashells. The plant was designed to process 10,886 MT of raw waste shells (SCS: QS, 1:1, w/w) per year. The annual operating time was assumed to be 330 days. Process models were developed for three quality levels, SQ1, SQ2, and SQ3, separately. The processing capacity and operation period were the same in all three cases. The key starting parameters applied in the process are

shown in Table S1.

2.5.1. Process model description

The process flow diagram (PFD) for SQ1 production is shown in Figure S2. Waste seashells collected from the seafood processing plant are weighed at the entrance, then sent to the washing area via a belt conveyor. A metal detector is used to identify metallic elements that pose risks to subsequent processes, especially grinding. Shells are washed with hot water at a ratio of 1:2 (w/w) in a rotary washing machine to remove impurities. Wastewater and mud waste go to the wastewater treatment plant. The cleaned shells are then sent to a hammer mill using a belt conveyor for the primary size reduction. Ground shells with particle sizes smaller than 0.84 mm are then boiled with hot water for one hour in a stirred reactor. The solid loading of the reactor was set to $\sim\!32$ %. After leaving the reactor, a sieve shaker was used to remove most of the water, any remaining water in the ground shells is leached out in the following belt conveying and waste separator. A ball mill is then used to further reduce the particle size of shells to $\sim\!44~\text{um}$.

During heating, the shells with fine particle sizes are first heated to 140 °C to remove water in a rotary dryer. Then the temperature of the shell particles is increased to around 160 °C in a heater, where the heat energy comes from a downstream cyclone 2. The temperature is ramped to 300 °C and maintained for 2 h in a rotary kiln. The gas generated during the heating process is filtered in a baghouse filter. Any particles removed from the gas stream are recycled into the main product stream. The calcined shells are then cooled to 60 °C in two consecutive steps: (1) injection of water into the shells to decrease the temperature from 300 °C to 180 °C; and (2) introduction of air to decrease the temperature to 60 °C. This process design of heating and cooling was conducted in the same manner as a previous reports (Barros et al., 2009). The cooled CaCO₃ product (SQ1) is sent to a roller mill before storing. This final grinding is designed to reduce any large particles that form during the heating and cooling process.

Natural gas was used as the sole energy source for hot water, drying, and heating. The process diagram for SQ2 production is like that of SQ1 production (**Figure S3**). Changes in the production of SQ2 include, no hot water washing for the primary ground shells, and the particle size of shells before heating is $\sim\!74\,\mu m$, which is 30 μm larger than the SQ1. SQ2 was cooled and ground before storing in the same manner as SQ1. The processing of SQ3 production is less complicated than that of SQ1 and SQ2 because there is no hot water washing for the fine ground shells and no heating (**Figure S4**). Therefore, after the primary size reduction using a hammer mill, the shells are sent to a ball mill to reduce the particle size to $\sim 44\,\mu m$. The finely ground shells are then dried at 105 °C to remove the remaining water in the product. The final grinder, a roller mill, was used to ensure that the final product has similar particle size distributions.

2.5.2. Total capital investment and annual operating costs

The SQ production from the seashells model used the default SuperPro methodology for estimating the costs, which is described in detail in the book entitled "Plant Design and Economics for Chemical Engineers" (Peters et al., 2003). For all economic calculations, the year 2022 was used and the currency was US dollars (\$). Direct fixed capital (DFC), working capital, and startup cost were considered when calculating the total capital investment. DFC includes total plant cost (direct & indirect), contractor's fee, and contingency. Total plant direct cost is composed of cost of equipment, installation, process piping, instrumentation, electrical, buildings, yard improvement, and auxiliary facilities. The total plant indirect cost includes engineering and construction expenses. Costs of specific equipment are obtained from references or vendor quotes. For the equipment with a different size, the cost was adjusted based on Eq. (2) (Humbird et al., 2011).

$$new\ cost = (base\ Cost) \left(\frac{new\ Size}{base\ size}\right)^n \tag{2}$$

Where, n is the scaling factor, usually in the range of 0.5 to 0.8 (Humbird et al., 2011). Costs of common and small equipment, such as pumps, fans, belts, heat exchangers, were calculated based on the built-in cost models of SuperPro Designer.

The operating costs accounted for in this study include raw materials, utilities, labor, laboratory/quality control (QC)/quality assurance (QA), consumables, waste treatment/disposal, and facility-dependent costs (including plant maintenance, depreciation, and overhead expenses). The prices of SCS and QS were set at 0 \$/MT since some seafood processing plants pay outside service partners to take the shell waste based on the survey. The prices of electricity (\$0.10/kWh), chilled water (\$0.05/MT), and some consumables utilized were the default values provided by SuperPro. The water price was set at \$0.35/MT of shells (Jin et al., 2021). Based on the industrial price of natural gas provided by the U.S. Energy Information Administration from January to May (United States Natural Gas Industrial Price, n.d.), the natural gas price was set at \$342/MT. The hourly labor cost was estimated based on the average wages of chemical equipment operators in the chemical manufacturing industry in the U.S.(US Bureau of Labor Statistics Hourly Mean Wage for Chemical Equipment Operators and Tenders in Chemical Manufacturing in the United States, n.d.). The laboratory/QC/QA was calculated at 15 % of the total labor cost.(Ferreira et al., 2021)

2.5.3. Revenues, profitability, and sensitivity analysis

The selling prices of SQ1, SQ2, and SQ3 were set at \$1.00, \$0.50, and \$0.20/kg, respectively, which were based on the bulk market prices (Alibaba.com). The market price of CaCO₃ is highly variable depending on the quality. The project lifetime was set as 15 years. The economic performance of the process was evaluated by net present value (NPV), internal rate of return (IRR), and payback period. NPV is the difference between the present values of cash inflows and outflows over time, and it was calculated by assuming the plant operating time of 15 years with a discount rate of 7 %. A positive NPV indicates that the proposed project is financially viable. When the NPV is equal to zero, the payback time is reached, indicating the investor can recover the cost of an investment. IRR is the discount rate that makes the NPV zero. A single-point sensitivity analysis was performed to test variables that were uncertain or significantly affect the NPV. The variables considered in this study included plant capacity, natural gas price, electricity price, the selling price of SQ products, plant operating time, NPV interest rate, and inflation.

3. Results and discussion

3.1. CaCO₃ production from SCS and QS in a lab-scale process

On the lab scale, Surf clam (SCS) and quahog (QS) shells were ground to different sizes then heated at different temperatures and the color and calcium carbonate content was evaluated; the combination that resulted in the whitest color and the highest calcium carbonate was selected for further studies. Shells at the millimeter, sub-millimeter and micron scales were heated at three different temperatures 300, 350 and 500 °C. Shells at the micron scale produced the whitest CaCO3 when heated to 300 or 350 °C. Heating at 500 °C produced a dark gray product. Because the goal of this project was to produce the lightest colored product with the highest CaCO3 content, we chose 300 °C as our heat treatment maximum as there was no improvement at 350 °C. Additional details of the conditions used and the resulting color and chemical composition of our products follow.

3.1.1. Color of CaCO₃ samples

Color is one of the primary quality indicators for CaCO3 and for its

industrial applications. Our goal, therefore, was to find the conditions that would produce the whitest product. Based on the preliminary experiment, heating at 500 °C for 1, 10, or 12 h, resulted in a permanently dark gray color of CaCO_3 for both coarsely ground (5–10 mm) and finely ground (0.5–5 mm) shells (**Figure S5**); for the same heating durations, 300 °C the samples were whiter than both 500 °C and 350 °C. The development of dark gray color of seashells at temperatures above 300 °C was also observed by Milano et al. (2016). They suggest that the color change might be due to the combustion of residual organic matter and shell charring.

Additionally, shell particle size reduction using ball milling before heating (300 °C) increased the brightness of the $CaCO_3$ product, such that the L* increased from 59.22 for the sample of only quahog shells that were ball milled after heating to an L* value of 72.95 for a second sample of only quahog shells that was ball milled before heating (Table S2). Similar results were found for samples of surf clam shells, ball milling before heating resulted in a whiter sample and a higher overall L* value. We postulate that increasing the surface area of the shells was helpful for removing the impurities during the heating process. The morphology and size of the ball-milled samples heated at 300 °C was evaluated using SEM (Figure S8). Samples that have been ball-milled and then heated to 300 °C, showed much better particular distribution in the sub-micron range with less agglomeration and whiteness (Table S2).

Based on this data, in the production of our final products, we controlled the particle sizes of shells at the micron level (44 or 74 μm) before heating. In addition, during the water boiling step, some small shell particles with dark coloration floated on top of the water and could be physically removed with the water. Therefore, in the optimized process, the shells were coarsely ground to particle sizes no larger than 0.84 mm, that could pass through mesh No. 20, before being sent to the water boiling process, then milled to the micron-scale using a coffee grinder prior to heating at 300 °C for 2 h. This low heating temperature is less energy-intensive compared to heating at higher temperatures, which is beneficial for the production plant, and the economy, but still produces a white product with high calcium carbonate content.

Because the seafood processing factories do not process only one kind of shell, we investigated a 1-to-1 w/w mixture of surf clam and quahog shells (SQ). We coarsely ground the cleaned shell mixture to particle sizes no larger than 0.84 mm, then boiled the shell mixture in water for 1 h. After which, the mixture was dried and finely ground to 74 μ m followed by heating at 300 °C for 2 h. The produced CaCO₃ had an L* value of 91.1, which indicated an overall white color, but in comparison to our standard CaCO₃, our SQ sample it was significantly less white (p < 0.0001). However, the color of the produced CaCO₃ is comparable to commercial CaCO₃ that is used in the paper and agricultural industries (*How Stone Paper is Made*, n.d.; *Huber Engineered Materials. Agriculture.*, n.d.), and although the color of CaCO₃ is not a high priority factor within the pet food industry, the CaCO₃ content and the whiteness of our products were within their standards (Panasevich, 2021).

3.1.2. XRF and XRD analysis of CaCO₃ samples

The results of XRF and elemental analysis indicated that the materials obtained from SCS and QS was primarily composed of CaCO $_3$ with minor other chemical components (**Table S3**). The results are in line with the literature reports (Chilakala et al., 2019) and matched our CaCO $_3$ control which, reported as CaO by convention, accounts for 53–55 % of the shell, meaning that the shell is > 95 % CaCO $_3$. In our study, there were slight differences in the amount of CaCO $_3$ depending on the sample preparation. The shells that were treated only with hot water (no ball milling or heating) elemental analysis showed a CaO composition between 48.8–49.8 %. Samples heated and then ball milled or ball milled then heated had slightly increased, but similar, CaO content in the product to 50.5–51.5 %, indicating that the decomposition of CaCO $_3$ was minimized at 300 °C. These values were only slightly

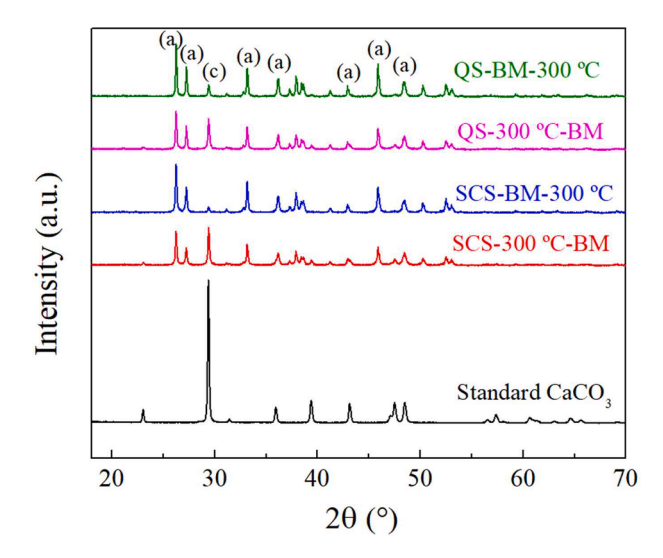


Fig. 2. The X-ray diffraction patterns of CaCO₃ samples were obtained from a lab-scale process. BM: ball milling. (a) Aragonite; (c): Calcite.

below the standard CaCO $_3$ material, and better than the reported numbers for higher heating temperatures (>500 °C) which led to a significant increase in CaO due to the decomposition of CaCO $_3$ to CaO before analysis (Mo et al., 2018).

The crystallinity of the CaCO3 products obtained from QS and SCS powder was evaluated using XRD. The major diffraction peaks for the crystalline structures in the powders are in the 20 range of 25-55° (Fig. 2). Products obtained from the same processing from QS and SCS shared similar XRD patterns. In combination with our XRF results (Table S3), we know that the powder products obtained from the QS and SCS processing is primarily CaCO₃. CaCO₃ is characterized by two natural crystal forms: aragonite and calcite. Therefore, the diffraction peaks of aragonite and calcite crystals are found in the powders obtained from seashells (Fombuena et al., 2014). The representative peaks of the aragonite peaks located at around 26°, 33° and 46° were shown in the XRD pattern of seashell powders, confirming that CaCO₃ in the seashell powders is mainly in the form of aragonite crystals, which is similar to other seashells, such as white clam shells (Liang et al., 2016) and green mussel shells (Suwannasingha et al., 2022). In our standard CaCO₃, there is an obvious peak at 29.4°, which corresponds to the calcite crystal that has been reported in oyster shells (Nguyen Quang and Ta Hong, 2022). The difference in the crystalline phases in various types of seashells could be a result of their organic matrices and other inorganic inclusions due to their growing environments (Suwannasingha et al., 2022). There is small but observable change in calcite crystal peak obtained at 29.4° when heat is followed by ball milling. This change in the prevalence of different crystal forms of CaCO3 from seashells with ball milling and heat treatment was reported by several researchers (Wu et al., 2011; Hussain and Sabiruddin, 2021). Particle size may affect the heat transfer within the samples, which in turn impacts the aragonite to calcite transition.

3.2. Production and characterization of grades of CaCO₃

Based on the lab-scale experiments, three different grades of $CaCO_3$, based on color and carbonate content, were obtained: SQ1, SQ2 and SQ3. Both SQ1 and SQ2 were heated to $300\,^{\circ}C$ with minor changes before heating but SQ3 was obtained directly from the initial washing and grinding step. Additional details of the conditions used, and the resulting color and chemical composition of our products follow.

3.2.1. Hunter color properties

The hunter color values (L* for lightness, a* for red/green, and b* for

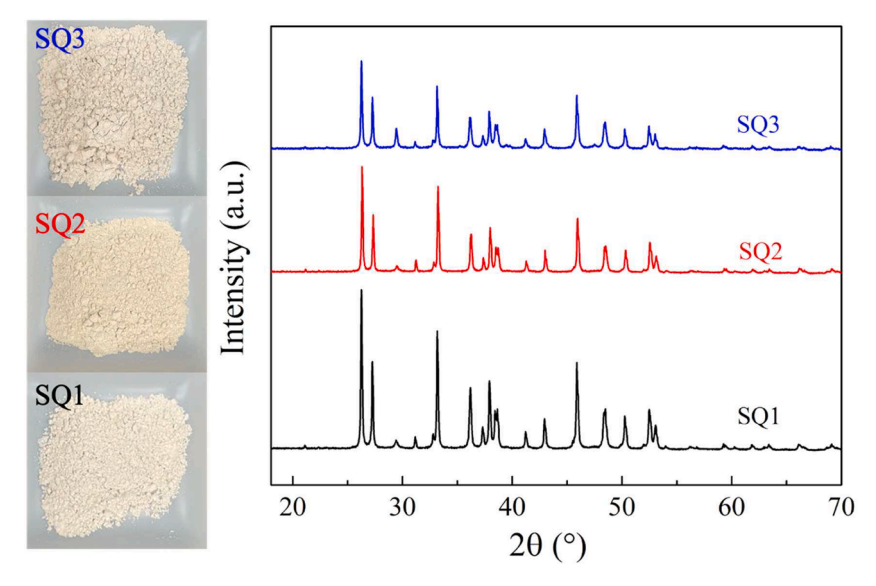


Fig. 3. (a) SQ products obtained from waste shells of Ocean quahog and Surf clam. Photo credit Peilong Li. (b) XRD of SQ1, SQ2 and SQ3 samples showing aragonite as the primary CaCO₃ form.

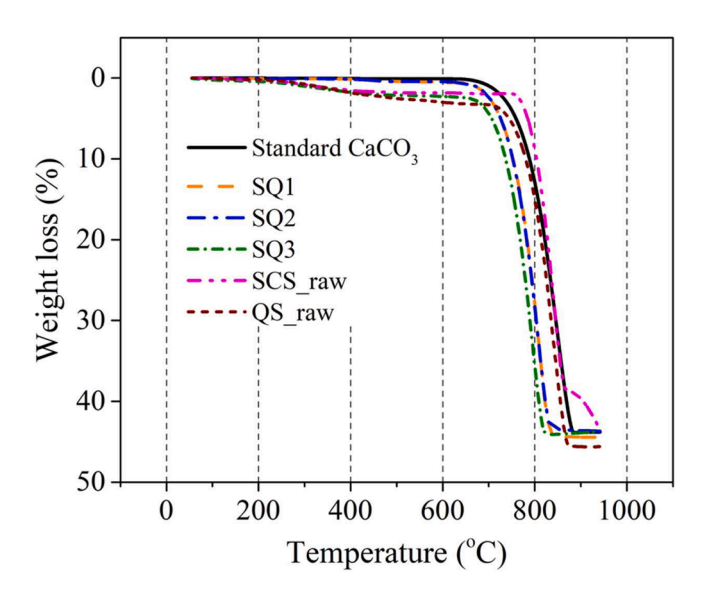


Fig. 4. Thermogravimetric analysis (TGA) curves of waste shells of surf clam and ocean quahog, and SQ products obtained from these shells.

yellow/blue) of these SQ products were compared to the standard CaCO $_3$. The SQ products were found to be less white (lower L*) and more yellow (higher b*) (Fig. 3 and Table S4). SQ1, which were ball milled, then had an additional boiling water wash before being heated at 300 °C, produced a CaCO $_3$ product with color values closest to the standard sample. SQ2 and SQ3 were noticeably darker, and their L* values reflected the change. SQ2, despite being heat treated at 300 °C, had the lowest L* value.

3.2.2. XRD and ATR-FTIR spectra

The XRD for the SQ products indicates that each of the SQ products have the same main diffraction peaks as the starting materials, where aragonite is the predominant crystal form (Fig. 3). The intensity of the peak at 29.4° , which corresponds to the calcite crystal form, is of highest intensity for SQ3, which was not heated at 300 °C. This difference is attributed to the heating process used to produce the SQ1 and SQ2. Overall, the heating temperature (300 °C) did not change the main crystal forms of resulting CaCO $_3$ products obtained.

An FTIR study was conducted to investigate the effect of processing on the functional groups of shell powders (**Figure S7**). The standard CaCO₃ presented three major bands at 1445, 870, and 714 cm $^{-1}$, and the major bands of SQ products were at 1440, 854, and 714 cm $^{-1}$. The bands in the region of 1400–1600 and 700–900 cm $^{-1}$ confirm the existence of the carbonate groups of CaCO₃ (Dhanaraj and Suresh, 2018; Ismail et al., 2021; Tămășan et al., 2013). One additional less obvious band appeared at 1080 cm $^{-1}$ of the SQ products corresponding to symmetric carbonate stretching vibration of aragonite (Mindivan and Göktaş, 2020). The results indicated that the hot water and heating did not affect the functional groups of the SQ samples; CaCO₃ in the shells did not decompose during the heating process.

3.2.3. Thermogravimetric analysis (TGA)

TGA was used to determine the fraction of volatile components by monitoring the weight change that occurs during heating of the SQ samples. We monitored weight loss from 25 °C to 950 °C of raw cleaned shells, SQ products, and standard CaCO3 (Fig. 4). The weight loss of samples occurred in three stages: (1) moisture evaporation (~ 125 °C); 2) organic release (125-650 °C); 3) CO₂ release (650-915 °C) (Ferraz et al., 2019). The major weight loss (~ 44 %) occurred during 650-915 °C for all the CaCO3 samples, indicating the thermal decomposition of CaCO3 into calcium oxide and carbon dioxide. The shells, SQ3, raw SCS and QS had ~2 % weight loss due to the organic mass release when the temperature increased from 125 °C to 650 °C, while the TGA pattern of SQ1, SQ2, and standard CaCO₃ showed less than 0.8 % weight loss. The results indicated the heat treatment (300 °C) was effective in removing the organic matter from SCS and QS. SQ1 had the same CaCO₃ content (99.3 %) as the standard sample, while the CaCO₃ contents of SQ2 and SQ3 were 97.4 % and 94.1 %, respectively. These results provided evidence that the identified optimized process, hot water wash combined with 300 °C treatment, improved the CaCO3 content of the product.

3.2.4. In vitro solubility, loose bulk density, and pH

Typical physical properties including vitro solubility, loose bulk density, and pH values are often reported for commercial calcium carbonate used in animal feed. Therefore, these properties of SQ products were evaluated (**Table S5**). The in vitro solubility of our SQ products was higher than 99 %, which is similar to the standard CaCO $_3$. There was no significant difference existing in the in vitro solubility and pH values among the SQ samples (p > 0.05). The loose bulk density of SQ1 and SQ3

Table 1Total capital investment in thousands of US dollars (\$ K) of SQ1, SQ2, and SQ3 production plants.

Item	SQ1 (US \$ K)	SQ2 (US \$ K)	SQ3 (US \$ K)
Direct fixed capital (DFC)			
Equipment purchase cost	2299	1696	961
Construction	2095	1582	832
Engineering	1496	1130	594
Equipment installation	1089	908	330
Contingency	958	723	380
Process piping	575	424	240
Contractor's fee	479	362	190
Instrumentation	460	339	192
Buildings	460	339	192
Auxiliary facilities	460	339	192
Yard improvement	345	254	144
Insulation and electrical	299	221	125
Sum of Direct fixed capital (DFC)	11,015	8317	4372
Working capital (WC)	439	328	247
Startup cost (SC)	551	416	219
Total capital investment (TCI = DFC $+$ WC $+$ SC)	12,005	9061	4838

were the same, 54 lbs/ft³, but for SQ2 the bulk density was 66 lbs/ft³. We attributed this to the difference in particle size. SQ1 and SQ3 share the same particle size, 44 μm , but the particle size of SQ2 was 74 μm . The small particle size of SQ1 and SQ3 provided a lower loose bulk density, which is in line with the commercial CaCO3 products.(Huber Engineered Materials. Agriculture., n.d.)

3.2.5. Elemental composition

The elemental composition of the SQ products was measured using ICP-MS (Table S6), ICP-MS was used to identify heavy metals in the SQ products and to ensure they are at safe levels. The calcium content of SQ products was around 36 %, which makes SQ comparable to commercial limestone (calcium content 36–38 %) which is used in livestock feeds (Data sheets: Calcium carbonate, n.d.; Limestone, n.d.). Some elements such as Al, P, Fe, K, Mn, Ni, and Zn in SQ3 were especially higher than those in SQ1, which might due to the hot water boiling and wash process for SQ1 production that removed some of these elements. The concentrations of heavy metals, including As, Cd, and Hg in SQ products were at safe levels according to FDA standards (Deemy et al., n.d.).

3.3. Techno-economic analysis of SQ production

Plant design based on the results obtained from the lab-scale and the scale up production for each of the three grades of $CaCO_3$ was done using SuperPro Designer software. These starting values, such as moisture

Table 2Economic indicators (NPV, IRR, and payback period), minimum selling prices of SQ products, minimum plant capacity, and maximum shell cost for SQ production.

Item	SQ1	SQ2 ^a	SQ3 ^a
Revenue (US \$ K/year)	9100	4700	2000
NPV (at 7 % interest, US \$ K/year)	4300	-12,500	-18,400
IRR (%)	12.7	ND^1	ND
Payback time (years)	5.6	ND	ND
Minimum selling price (US \$/kg)	0.92	0.69	0.44
Minimum plant capacity (MT/year)	9889	15,756	27,045
Maximum shell cost (US-\$/MT)	67.4	< 0	< 0

^a ND indicates not determined. The negative NPV indicates the investments for plants are economically unfeasible, therefore, the IRR and payback time was not determined.

content of raw shells, water usage ratio, retention time of hot water wash and rotary kiln, $CaCO_3$ content and yields of SQ1, SQ2, and SQ3, were used as the initial simulation starting points (**Table S1**; for details of mass flow see **Figure S9**). The process simulation was used to estimate the economic feasibility of producing different grades of $CaCO_3$ and details of the study and the output from the process simulation are discussed.

3.3.1. Total capital investment of industrial plant

Based on the generated economic evaluation report from SuperPro Designer, the estimated total capital investment (TCI) of plants with an annual processing capacity of 10,886 MT of waste SCS and QS was estimated for SQ1 to be \$12.0 M (million), \$9.1 M for SQ2, and \$4.8 M for SQ3 (Table 1). The equipment cost was the major contributor to the TCI for all three plants. The SQ1 plant had the highest purchased equipment cost, \$2.3 M, due to the quantity of equipment required to wash the milled shells.

3.3.2. Annual operating cost of plants

The annual operating costs of each of the plants was estimated to be: SQ1, \$7.59 M; SQ2, \$5.70 M; and SQ3 \$3.92 M (Fig. 5). The labor-dependent costs contributed the most to the operating cost (more than 56 %), followed by facility-dependent costs, such as depreciation, maintenance, insurance, and overhead, for all three plants. Therefore, improving plant automation or the use of artificial intelligence such as robots provide possibilities could reduce costs. Utilities, including water, natural gas, and electricity, accounted for 4–6 % of total operating cost. The distribution of annual operating costs of plants SQ1 and SQ2 was similar due to the equipment intense heating step, which the SQ3 plant does not have. The consumables cost was negligible (<0.1 %), especially for the SQ3 plant.

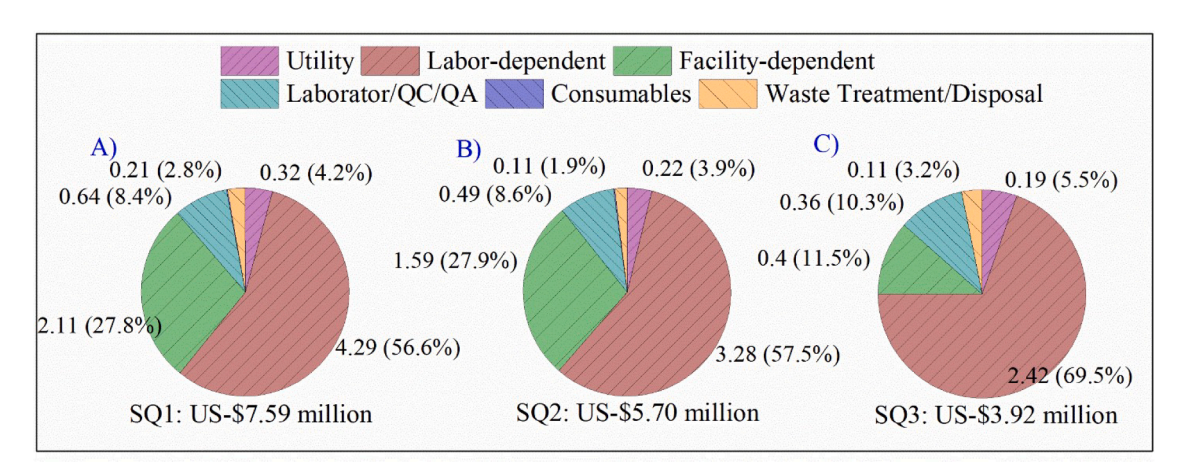


Fig. 5. Annual operating cost and distribution of plants for SQ1, SQ2, and SQ3 production.

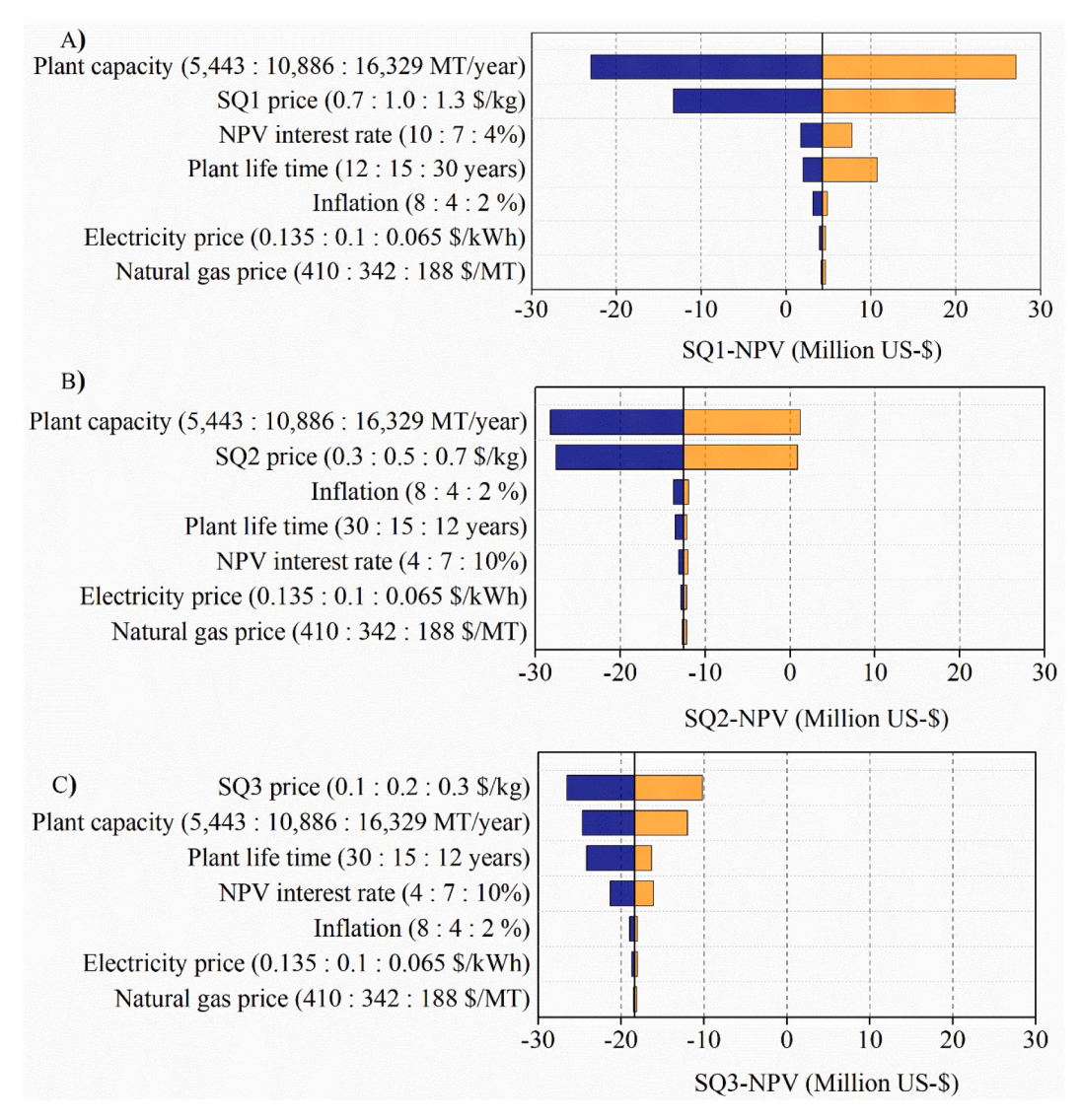


Fig. 6. Sensitivity of NPV in millions of US dollars (\$ M) of different parameters for CaCO3 products (\$Q) production from waste seashells.

3.3.3. Revenue and profitability of plants

The processing capacity of the three plants was set at 10,886 MT of shells/year, and the production capacity of SQ1, SQ2, and SQ3 was 9078, 9357, and 9508 MT/year, respectively. The unit production cost of SQ3 was \$0.41/kg, which is lower than that of SQ2 (\$0.61/kg) and SQ1 (\$0.84/kg). Considering the selling prices of SQ1 (\$1.00/kg), SQ2 (\$0.50/kg), and SQ3 (\$0.20/kg), the total annual revenues obtained from the corresponding plants would be \$9.1 M/year for SQ1, \$4.7 M/year for SQ2, and \$2.0 M/year for SQ3 (Table 2). Even with the higher production costs associated with SQ1, the higher selling price still allowed for a higher revenue than SQ2 and SQ3.

The economic performance of the processes for SQ production was evaluated by NPV, IRR, and payback period (Table 2). The IRR for SQ1 was 12.7 %, with an NPV of \$4.3 M and a payback time of 5.6 years. The positive NPV indicates an economically feasible investment for SQ1 production, since the NPV of the SQ2 and SQ3 plants was negative; investments in the production plans for SQ2 and SQ3 would result in a net loss over the plant lifetime and therefore unfeasible.

Based on the sensitivity analysis (Fig. 6), the variations in plant capacity and SQ selling price played important roles in NPV. The minimum selling price of the SQ products and minimum plant capacities were estimated by calculating NPV to zero (Table 2). As to the SQ1 plant, when the SQ1 price is not less than \$0.92/kg or plant production is

greater than 9889 MT/year, the SQ1 plant will be economically feasible. To be feasible, the selling prices for SQ2 and SQ3 need to be higher than 0.69kg and 0.44kg, respectively, and the plant capacity would need to be increased to 0.5756 MT/year for SQ2 and 0.7045 MT/year for SQ3.

We set the cost of shells to \$0/MT in our base models and proposed that our plants would be co-located near seafood processing plants. We considered that although the costs of shells may remain zero, there may be associated transportation costs. Therefore, one possible scenario included designing an SQ plant that would require transportation of the shells even though the purchase cost of shells is zero. Based on the calculation of NPV equaling zero (Table 2), the maximum cost of transported shells could be \$67.4/MT, while SQ1 will remain feasible under this burden, any cost associated with shell transport for the SQ2 and SQ3 plants, however, makes the investment in these plants economically unfavorable.

3.3.4. Sensitivity analysis

Economically, SQ production is based on various factors that determine the profitability of plants. A single-point sensitivity analysis was used to test several variables that were uncertain or affected NPV. Both low- and high-end values of the variables were selected based on previous studies (He et al., 2021; Jin et al., 2021) or set as ± 20 –50 % of the base value (Zang et al., 2020). The sensitivity analysis results of

production plants for SQ1, SQ2, and SQ3 show that the plant capacity and selling prices of SQ products play a key in determining the NPV (Fig. 6A, B and C). For plants SQ1 and SQ2, the plant capacity was the dominant parameter influencing the NPV. Increasing the plant capacity of SQ1 from 10,886 to 16,329 MT/year (50 % increase), leading to a 533.8 % increase in NPV, while scaling down the plant capacity to 5443 MT/year resulted in the NPV decreasing from \$4.3 M to -\$23.0 M. Similarly, for the SQ2 plant, the NPV changed from -\$28.2 M to positive \$1.2 M when the plant capacity increased from 5443 to 16,329 MT/year. While plant capacity was the second key factor affecting the NPV of the SQ3 plant, and regardless of the scale of its plant capacity, the NPV of SQ3 plant was always negative.

The SQ1 selling price was the second major variable that influenced the NPV. Within the selling price of SQ1 changing from \$0.7/kg to \$1.3/kg, the NPV changed from -\$13.3 M to \$19.9 M. The 40 % increase or decrease in the SQ2 selling price increased the NPV by 107 % or decreased by 120 %. Compared to SQ1 and SQ2, the price of SQ3 was the predominant factor that affected the NPV, followed by the plant capacity. However, the NPV of SQ3 plant was negative even when the selling price of SQ3 increased to \$0.3/kg. Plant lifetime and NPV interest rate were the other factors that could affect the NPV of plants SQ1 and SQ3. The price of natural gas also fluctuates, but its effect on the NPV was small for all the three plants. For the SQ3 plant, the NPV was always negative.

4. Conclusions

This study reported an environmentally friendly process that combined a hot water wash, ball milling and heating at 300 °C to produce high-quality CaCO₃ from waste surf clam (SCS) and ocean quahog (QS) shells. Three processes were designed to produce three grades of CaCO₃ products: SQ1, SQ2, and SQ3, using the mixture of SCS and QS as a raw material. SQ1 is white and contains 99.3 % of CaCO₃. Considering the different market requirements for CaCO3 products, processing designs for producing SQ2 with white color but lower CaCO₃ content (97.4 %), and SQ3 with less white color and lower CaCO3 content of 94.1 % were developed. The identified processing conditions were further verified by scaled-up processing. The techno-economic models of SQ1, SQ2, and SQ3 production indicated that SQ1 production is economically feasible while no realistic model for SQ2 and SQ3 was found. The IRR for SQ1 was 12.7 %, with an NPV of \$4.3 M and a payback time of 5.6 years. Sensitivity analysis showed that plant capacity and the selling price of SQ1 had the most impact on the economic performance of the SQ1 plant. Overall, the study demonstrated that producing high-quality CaCO₃ products from waste seashells is technically and economically feasible.

CRediT authorship contribution statement

Yanhong He: Conceptualization, Investigation, Data curation, Formal analysis, Methodology, Writing – original draft, Writing – review & editing. Mojtaba Enayati: Conceptualization, Investigation, Data curation, Formal analysis, Methodology, Writing – original draft, Writing – review & editing. Younas Dadmohammadi: Conceptualization, Supervision, Writing – review & editing. Martin Liu: Investigation, Data curation, Writing – review & editing. Peilong Li: Investigation, Data curation, Writing – review & editing. Alireza Abbaspourrad: Conceptualization, Supervision, Funding acquisition, Project administration, Writing – review & editing.

Declaration of Competing Interest

The authors declare that they have no known competing financial interests or personal relationships that could have appeared to influence the work reported in this paper.

Data availability

Data will be made available on request.

Acknowledgments

This work was supported by the National Science Foundation (PTE Federal Award No:1841112) and made use of the Cornell Center for Materials Research Shared Facilities which are supported through the NSF MRSEC program (DMR-1719875). We would like to acknowledge Surfside Foods LLC (NJ), Atlantic Capes Fisheries, Inc. (NJ), La Monica Fine Foods (NJ), Sea Watch International, Ltd. (MD) for providing shells, and Harrop Industries, Inc (Columbus, OH, USA) for helping to prepare CaCO₃ samples. We thank McAlister Council-Troche (VetMed Analytical Research Lab, Virginia Tech) for his help in the ICP-MS analysis, and Warren Straszherim (Materials Analysis and Research Lab, Iowa State University) for his help in the XRF analysis. Nik Misailidis and Demetri Petrides (Intelligen, Inc) assisted with the model design simulation. We thank Cornell Management Library, especially Susan F. Kendrick and Tom J. Ottaviano, for providing information about the CaCO₃ market report.

Supplementary materials

Supplementary material associated with this article can be found, in the online version, at doi:10.1016/j.rcradv.2023.200190.

References

- Águila-Almanza, E., Hernández-Cocoletzi, H., Rubio-Rosas, E., Calleja-González, M., Lim, H.R., Khoo, K.S., Singh, V., Maldonado-Montiel, J.C., Show, P.L., 2022. Recuperation and characterization of calcium carbonate from residual oyster and clamshells and their incorporation into a residential finish. Chemosphere 288, 132550. https://doi.org/10.1016/j.chemosphere.2021.132550.
- Aimikhe, V., Lekia, G., 2021. An overview of the applications of periwinkle (Tympanotonus fuscatus) shells. Curr. J. Appl. Sci. Technol. 40, 31–58. https://doi. org/10.9734/CJAST/2021/v40i1831442.
- ASTM C25, 2021. Standard Test Methods For Chemical Analysis of limestone, quicklime, and Hydrated Lime. www.astm.org (accessed 2021-11-20).
- Barros, M.C., Bello, P.M., Bao, M., Torrado, J.J., 2009. From waste to commodity: transforming shells into high purity calcium carbonate. J. Clean. Prod. Sustain. Seafood Prod. Consump. 17, 400–407. https://doi.org/10.1016/j. jclepro.2008.08.013.
- Chilakala, R., Thannaree, C., Shin, E.J., Thenepalli, T., Ahn, J.W., 2019. Sustainable solutions for oyster shell waste recycling in Thailand and the Philippines. Recycling 4, 35. https://doi.org/10.3390/recycling4030035.
- Dhanaraj, K., Suresh, G., 2018. Conversion of waste sea shell (Anadara Granosa) into valuable nanohydroxyapatite (NHAp) for biomedical applications. Vacuum 152, 222–230. https://doi.org/10.1016/j.vacuum.2018.03.021.
- Ferraz, E., Gamelas, J.A.F., Coroado, J., Monteiro, C., Rocha, F., 2019. Recycling waste seashells to produce calcitic lime: characterization and wet slaking reactivity. Waste Biomass Valor. 10, 2397–2414. https://doi.org/10.1007/s12649-018-0232-y.
- Ferreira, R.G., Azzoni, A.R., Santana, M.H.A., Petrides, D., 2021. Techno-economic analysis of a hyaluronic acid production process utilizing streptococcal fermentation. Processes 9, 241. https://doi.org/10.3390/pr9020241.
- Fisheries, N., 2022. Behind the Scenes of the Most Consumed Seafood | NOAA Fisheries [WWW Document]. NOAA. URL. https://www.fisheries.noaa.gov/feature-story/behind-scenes-most-consumed-seafood. accessed 7.20.22.
- Fombuena, V., Bernardi, L., Fenollar, O., Boronat, T., Balart, R., 2014. Characterization of green composites from biobased epoxy matrices and bio-fillers derived from seashell wastes. Mater. Design 57, 168–174. https://doi.org/10.1016/j. matdes.2013.12.032.
- Ganapathi, H., Phukan, M., 2020. Environmental hazards of limestone mining and adaptive practices for environment management plan. In: Singh, R.M., Shukla, P., Singh, P. (Eds.), Environmental Processes and Management: Tools and Practices, Water Science and Technology Library. Springer International Publishing, Cham, pp. 121–134. https://doi.org/10.1007/978-3-030-38152-3
- Hamester, M.R.R., Balzer, P.S., Becker, D., 2012. Characterization of calcium carbonate obtained from oyster and mussel shells and incorporation in polypropylene. Mat. Res. 15, 204–208. https://doi.org/10.1590/S1516-14392012005000014.
- He, Y., Kuhn, D.D., O'Keefe, S.F., Ogejo, J.A., Fraguas, C.F., Wang, H., Huang, H., 2021. Protein production from brewer's spent grain via wet fractionation: process optimization and techno-economic analysis. Food Bioprod. Process. 126, 234–244. https://doi.org/10.1016/j.fbp.2021.01.005.
- Hembrick-Holloman, V., Samuel, T., Mohammed, Z., Jeelani, S., Rangari, V.K., 2020. Ecofriendly production of bioactive tissue engineering scaffolds derived from egg-

- and sea-shells. J. Mater. Res. Technol. 9, 13729-13739. https://doi.org/10.1016/j.
- Humbird, D., Davis, R., Tao, L., Kinchin, C., Hsu, D., Aden, A., Schoen, P., Lukas, J., Olthof, B., Worley, M., 2011. Process Design and Economics for Biochemical Conversion of Lignocellulosic Biomass to Ethanol: Dilute-acid Pretreatment and Enzymatic Hydrolysis of Corn Stover. National Renewable Energy Lab.(NREL), Golden. COUnited States.
- Hussain, S., Sabiruddin, K., 2021. Effect of heat treatment on the synthesis of hydroxyapatite from Indian clam seashell by hydrothermal method. Ceram Int 47, 29660–29669. https://doi.org/10.1016/j.ceramint.2021.07.137.
- Ismail, R., Fitriyana, D.F., Santosa, Y.I., Nugroho, S., Hakim, A.J., Al Mulqi, Jamari, J., Bayuseno, A.P., 2021. The potential use of green mussel (Perna Viridis) shells for synthetic calcium carbonate polymorphs in biomaterials. J. Cryst. Growth 572, 126282. https://doi.org/10.1016/j.jcrysgro.2021.126282.
- Jin, Q., O'Keefe, S.F., Stewart, A.C., Neilson, A.P., Kim, Y.-T., Huang, H., 2021. Technoeconomic analysis of a grape pomace biorefinery: Production of seed oil, polyphenols, and biochar. Food Bioprod. Process. 127, 139–151. https://doi.org/ 10.1016/j.fbp.2021.02.002.
- Kim, S.-W., Li, W., Angel, R., Proszkowiec-Weglarz, M., 2018. Effects of limestone particle size and dietary Ca concentration on apparent P and Ca digestibility in the presence or absence of phytase. Poultry Sci. 97, 4306–4314. https://doi.org/ 10.3382/ps/pey304.
- Liang, Y., Zhao, Q., Li, X., Zhang, Z., Ren, L., 2016. Study of the microstructure and mechanical properties of white clam shell. Micron 87, 10–17. https://doi.org/ 10.1016/j.micron.2016.04.007.
- Lin, P.-Y., Wu, H.-M., Hsieh, S.-L., Li, J.-S., Dong, C., Chen, C.-W., Hsieh, S., 2020. Preparation of vaterite calcium carbonate granules from discarded oyster shells as an adsorbent for heavy metal ions removal. Chemosphere 254, 126903. https://doi.org/10.1016/j.chemosphere.2020.126903.
- Milano, S., Prendergast, A.L., Schöne, B.R., 2016. Effects of cooking on mollusk shell structure and chemistry: Implications for archeology and paleoenvironmental reconstruction. J. Archaeol. Sci. Rep. 7, 14–26. https://doi.org/10.1016/j. jasrep.2016.03.045.
- Mindivan, F., Göktas, M., 2020. Production and Characterization of Graphene/PVC Biocomposite from Seashell Wastes. Mater Today: Proc 27, 3119–3123. https://doi. org/10.1016/j.matpr.2020.03.728.
- Mo, K.H., Alengaram, U.J., Jumaat, M.Z., Lee, S.C., Goh, W.I., Yuen, C.W., 2018. Recycling of seashell waste in concrete: a review. Constr. Build. Mater. 162, 751–764. https://doi.org/10.1016/j.conbuildmat.2017.12.009.
- Nguyen Quang, B., Ta Hong, D., 2022. Synthesis and characterization of feed-grade monocalcium phosphate Ca(H₂PO₄)₂·H₂O from oyster shell. J. Chem. 2022, e3821717 https://doi.org/10.1155/2022/3821717.
- M. Panasevich, Blue Buffalo Co., Ltd, personal communication. 2021.
- Peters, M.S., Timmerhaus, K.D., West, R.E., 2003. Plant Design and Economics For Chemical Engineers, 4. McGraw-Hill, New York. ISBN: 9780072392661.

- Prihanto, A., Muryanto, S., Ismail, R., Jamari, J., Bayuseno, A.P., 2022. Practical insights into the recycling of green mussel shells (Perna Viridis) for the production of precipitated calcium carbonate. Environ. Technol. 0, 1–11. https://doi.org/ 10.1080/09593330.2022.2103458.
- ReportLinker, 2022. Global Calcium Carbonate Market to Reach US\$28.9 Billion by the Year 2026 [WWW Document]. GlobeNewswire News Room. URL. https://www.globenewswire.com/en/news-release/2022/06/17/2464781/0/en/Global-Calcium-Carbonate-Market-to-Reach-US-28-9-Billion-by-the-Year-2026.html. accessed 7.14.22
- Summa, D., Lanzoni, M., Castaldelli, G., Fano, E.A., Tamburini, E., 2022. Trends and opportunities of bivalve shells' waste valorization in a prospect of circular blue bioeconomy. Resources 11, 48. https://doi.org/10.3390/resources11050048.
- Suwannasingha, N., Kantavong, A., Tunkijjanukij, S., Aenglong, C., Liu, H.-B., Klaypradit, W., 2022. Effect of calcination temperature on structure and characteristics of calcium oxide powder derived from marine shell waste. J. Saudi Chem. Soc. 26, 101441 https://doi.org/10.1016/j.jscs.2022.101441.
- Tămăşan, M., Ozyegin, L.S., Oktar, F.N., Simon, V., 2013. Characterization of calcium phosphate powders originating from phyllacanthus imperialis and trochidae infundibulum concavus marine shells. Mater Sci Eng. C 33 (5), 2569–2577. https://doi.org/10.1016/j.msec.2013.02.019.
- Tayeh, B.A., Hasaniyah, M.W., Zeyad, A.M., Yusuf, M.O., 2019. Properties of concrete containing recycled seashells as cement partial replacement: a review. J. Clean. Prod. 237, 117723 https://doi.org/10.1016/j.jclepro.2019.117723.
- The State of World Fisheries and Aquaculture 2022, 2022. FAO. https://doi.org/
- Wang, J.J., Liu, E., 2020. Upcycling waste seashells with cement: Rheology and early-age properties of Portland cement paste. Resour Conserv Recycl 155, 104680. https:// doi.org/10.1016/j.resconrec.2020.104680.
- Wijsman, J.W.M., Troost, K., Fang, J., Roncarati, A., 2019. Global production of marine bivalves. Trends and challenges. In: Smaal, A.C., Ferreira, J.G., Grant, J., Petersen, J. K., Strand, Ø. (Eds.), Goods and Services of Marine Bivalves. Springer International Publishing, Cham, pp. 7–26. https://doi.org/10.1007/978-3-319-96776-9_2.
- Wu, S.C., Hsu, H.C., Wu, Y.N., Ho, W.F., 2011. Hydroxyapatite synthesized from oyster shell powders by ball milling and heat treatment. Mater. Charact. 62 (12), 1180–1187. https://doi.org/10.1016/j.matchar.2011.09.009.
- Yadav, V.K., Yadav, K.K., Cabral-Pinto, M.M.S., Choudhary, N., Gnanamoorthy, G., Tirth, V., Prasad, S., Khan, A.H., Islam, S., Khan, N.A., 2021. The processing of calcium rich agricultural and industrial waste for recovery of calcium carbonate and calcium oxide and their application for environmental cleanup: a review. Appl. Sci. 11, 4212. https://doi.org/10.3390/app11094212.
- Yan, N., Chen, X., 2015. Sustainability: don't waste seafood waste. Nature 524, 155–157. https://doi.org/10.1038/524155a.
- Zang, G., Shah, A., Wan, C., 2020. Techno-economic analysis of an integrated biorefinery strategy based on one-pot biomass fractionation and furfural production. J. Clean. Prod. 260, 120837 https://doi.org/10.1016/j.jclepro.2020.120837.